Global Change Biology

Global Change Biology (2015), doi: 10.1111/gcb.12795

Detection and attribution of vegetation greening trend in China over the last 30 years

SHILONG PIAO[1,2], GUODONG YIN[1], JIANGUANG TAN[1], LEI CHENG[3], MENGTIAN HUANG[1], YUE LI[1], RONGGAO LIU[4], JIAFU MAO[5], RANGA B MYNENI[6], SHUSHI PENG[1], BEN POULTER[7], XIAOYING SHI[4], ZHIQIANG XIAO[8], NING ZENG[9], ZHENZHONG ZENG[1] and YINGPING WANG[3]

[1]*Sino-French Institute for Earth System Science, College of Urban and Environmental Sciences, Peking University, Beijing 100871, China,* [2]*Institute of Tibetan Plateau Research, Center for Excellence in Tibetan Earth Scicence, Chinese Academy of Sciences, Beijing 100085, China,* [3]*CSIRO Marine and Atmospheric Research, Centre for Australian Weather and Climate Research, PMB #1, Aspendale, Vic. 3195, Australia,* [4]*Institute of Geographic Sciences and Natural Resources Research, Chinese Academy of Sciences, Beijing, 100101, China,* [5]*Climate Change Science Institute and Environmental Sciences Division, Oak Ridge National Laboratory, Oak Ridge, TN, USA,* [6]*Department of Earth and Environment, Boston University, 675 Commonwealth Avenue, Boston, MA 02215, USA,* [7]*Institute on Ecosystems and the Department of Ecology, Montana State University, Bozeman, MT 59717, USA,* [8]*School of Geography, Beijing Normal University, Beijing 100875, China,* [9] *Department of Atmospheric and Oceanic Science, University of Maryland, College Park, MD 20740, USA*

Abstract

The reliable detection and attribution of changes in vegetation growth is a prerequisite for the development of strategies for the sustainable management of ecosystems. This is an extraordinary challenge. To our knowledge, this study is the first to comprehensively detect and attribute a greening trend in China over the last three decades. We use three different satellite-derived Leaf Area Index (LAI) datasets for detection as well as five different process-based ecosystem models for attribution. Rising atmospheric CO_2 concentration and nitrogen deposition are identified as the most likely causes of the greening trend in China, explaining 85% and 41% of the average growing-season LAI trend (LAI_{GS}) estimated by satellite datasets (average trend of 0.0070 yr^{-1}, ranging from 0.0035 yr^{-1} to 0.0127 yr^{-1}), respectively. The contribution of nitrogen deposition is more clearly seen in southern China than in the north of the country. Models disagree about the contribution of climate change alone to the trend in LAI_{GS} at the country scale (one model shows a significant increasing trend, whereas two others show significant decreasing trends). However, the models generally agree on the negative impacts of climate change in north China and Inner Mongolia and the positive impact in the Qinghai–Xizang plateau. Provincial forest area change tends to be significantly correlated with the trend of LAI_{GS} ($P < 0.05$), and marginally significantly ($P = 0.07$) correlated with the residual of LAI_{GS} trend, calculated as the trend observed by satellite minus that estimated by models through considering the effects of climate change, rising CO_2 concentration and nitrogen deposition, across different provinces. This result highlights the important role of China's afforestation program in explaining the spatial patterns of trend in vegetation growth.

Keywords: afforestation, attribution, China, CO2 fertilization effect, detection, greening trend, nitrogen deposition

Received 18 August 2014 and accepted 16 October 2014

Introduction

Vegetation growth is strongly influenced by climate and climate change (Zhou *et al.*, 2001; Nemani *et al.*, 2003; Xu *et al.*, 2013) and can affect the climate system through a number of bio-physical processes (Friedlingstein *et al.*, 2006; Lee *et al.*, 2011; Peng *et al.*, 2014). As a result, monitoring, understanding and predicting the response of vegetation growth to global change has been a central activity in Earth system science during the past two decades. Repeated and long-term space-borne measurements of the Normalized Difference Vegetation Index (NDVI) by NOAA satellites show an unambiguous greening trend in China since 1982 (Piao *et al.*, 2003). This enhanced vegetation growth in China plays an important role in the global carbon cycle through the net accumulation of 0.18–0.26 Pg of carbon per year (Piao *et al.*, 2009), which is about 28–37% of the total fossil fuel emission from China over the last decade. Nevertheless, many aspects of vegetation dynamics in China still remain poorly understood. A critical gap in our understanding pertains to the attribution of this greening trend – if we do not understand the mechanisms for this trend we will have little confidence in our ability to accurately predict either its future evolution or the consequent impact on land carbon uptake in China.

Correspondence: Shilong Piao, tel. +86 10 6276 5578, fax 86 10 6275-6560, e-mail: slpiao@pku.edu.cn

Over the last few decades China has experienced remarkable climatic warming (Piao *et al.*, 2010). It has been suggested that this warming has stimulated vegetation growth both through extending the growing season and through promoting summer photosynthesis, particularly in regions where water is nonlimiting (Niemand *et al.*, 2005; Piao *et al.*, 2007, 2008). Moreover, the fertilization effects of rising atmospheric CO_2 concentration and atmospheric nitrogen (N) deposition have also been considered as possible drivers for the greening. Nitrogen deposition has increased across nearly all of China with average increases of 25% during 1990s and 2000s (Jia *et al.*, 2014). In addition to the change in climate and atmospheric composition, land-use change such as afforestation and reforestation may also have played a very important role. Based on the latest national forest inventory, China's forest area has increased by about 3.1×10^5 km^2 from the early 1980s (1977–1981) to the early 2010s (2004–2008) (Guo *et al.*, 2013). Several studies have also emphasized the potential role of increased crop production resulting from the modernization of agriculture (Huang *et al.*, 2007) and vegetation recovery in rural areas arising from the change in energy production systems and movement of the rural population to cities on the carbon sink of China (Piao *et al.*, 2009).

It is quite difficult to quantify the individual contributions of each of these driving factors to the observed greening trend in China. Statistical correlation or regression analysis has been used (e.g., Zhou *et al.*, 2001; Peng *et al.*, 2013), but they suffer from two potential limitations. Firstly, statistical analysis of historical data generally characterizes the main driving factors of temporal change in vegetation growth, and thus includes the signal not only from temporal trend, but also from interannual or decadal variability (Ahlbeck, 2002). It should be noted that the dominant driving factors of temporal trend in vegetation growth may be different from that of interannual variability. For example, Piao *et al.* (2006) has suggested that at the continental scale, interannual variation in vegetation growth of the northern hemisphere is mainly driven by temperature variation, while rising CO_2 is the main contributor of the increasing trend in vegetation growth during the 1980s and 1990s. Another important caveat is that statistical analyses generally assume that effects of environmental variables on vegetation growth are linear and independent of each other. A growing body of evidence from both field experiment and theoretical analysis, however, shows nonlinear ecosystem responses to the environmental perturbations and changes (Berry & Bjorkman, 1980; Peng *et al.*, 2013; Yamori *et al.*, 2014, Piao *et al.*, 2014), highlighting the potential bias from a linear statistical analysis. Yet, these limitations are being overcome through the application of process-based ecosystem models driven by observed historical environmental variables (Hegerl *et al.*, 2010). For example, a recent study by Mao *et al.* (2012) has explored the cause of vegetation growth trend in the Northern Hemisphere from 1982 to 2004 using a process-based ecosystem model, CLM4 (Community Land Model version 4, Oleson *et al.*, 2010). A core limitation in the ecosystem model based approach is, however, the large uncertainties arising from model structure and parameter choices (Sitch *et al.*, 2008; Piao *et al.*, 2013). One of methods for quantifying those uncertainties is to use results from multiple models.

The primary objective of this study is to quantify the trend in vegetation greening in China during the last three decades, and to quantify the contributions from different factors including climate change, rising atmospheric CO_2 concentration, nitrogen deposition and afforestation. The study is based on satellite data and process-based ecosystem models. The degree of vegetation growth is inferred from the average leaf area index (LAI) during the growing season (defined as April to October) (LAI_{GS}). To reduce the uncertainty in our estimates of LAI, we apply three different satellite LAI datasets (GIMMS3 g (Zhu *et al.*, 2013), GLOBMAP (Liu *et al.*, 2012) and GLASS (Xiao *et al.*, 2014)), and five different process-based ecosystem models (CLM4 (Oleson *et al.*, 2010), CABLE (Wang *et al.*, 2010), ORCHIDEE (Krinner *et al.*, 2005), LPJ (Sitch *et al.*, 2003) and VEGAS (Zeng *et al.*, 2005)). First, we assess change in LAI_{GS} from three different satellite datasets to detect and characterize vegetation greening trend from 1982 to 2009. Second, we compare LAI_{GS} trend simulated by five process-based ecosystem models under different scenarios to the satellite-based measurements. This allows us to separate the contributions from each factor. Finally, we discuss the potential contribution of afforestation by analysing the spatial relationship of change in forest area reported by China's forest inventory data (Guo *et al.*, 2013) with the difference of LAI_{GS} trend between satellite and model estimates at provincial scale. Due to the lack of detailed information on the spatio-temporal change in land use, no models include land-use change in their simulations for this study.

Materials and methods

Satellite-derived LAI datasets

Remote sensing provides consistent measurements of LAI across large spatial and temporal ranges, and thus satellite-derived LAI datasets have been widely used for monitoring terrestrial vegetation growth at regional and global scales (Myneni *et al.*, 1997). In this study, three available satellite-derived LAI datasets are used to assess vegetation growth changes in China during the last three decades.

GIMMS LAI datasets. The Global Inventory Modeling and Mapping Studies (GIMMS) LAI is derived based on the third generation of Normalized Difference Vegetation Index (NDVI3 g) from GIMMS group and an Artificial Neural Network (ANN) model (Zhu *et al*., 2013). The temporal resolution of this dataset is half a month with one-twelfth of a degree spatial resolution. The quality of this dataset has been assessed through a series of tests and the results indicate suitability of the data for research use (Zhu *et al*., 2013).

GLOBMAP LAI datasets. GLOBMAP LAI is constructed by fusing Advanced Very High Resolution Radiometer (AVHRR) LAI (1981–2000) and MODIS LAI (2000–2011) (Liu *et al*., 2012). The AVHRR LAI during 1981–2000 is estimated using relationships between AVHRR observations and MODIS LAI at each pixel during the overlapping period (2000–2006). The temporal resolution of the GLOBMAP LAI dataset is the same as that of GIMMS LAI datasets, while the spatial resolution is 8 km.

GLASS LAI datasets. The Global Land Surface Satellite (GLASS) LAI product is generated from MODIS and AVHRR time-series reflectance data using general regression neural networks (Xiao *et al*., 2014). The temporal resolution of this dataset is 8 days. From 1981 to 1999, the LAI product is generated from LTDR AVHRR reflectance data. It is provided in a geographic latitude/longitude projection at a spatial resolution of 0.05° (about 5 km at the Equator). From 2000 to 2013, the LAI product is derived from MODIS surface-reflectance data. It is provided in a sinusoidal projection at a spatial resolution of 1 km. Extensive validation guarantees the method's qualification to estimate temporally and spatially continuous fields of LAI with much improved accuracy (Xiao *et al*., 2014).

Process-based ecosystem models

Over the last two decades, process-based ecosystem models have been developed that simulate the key processes (e.g., photosynthesis, respiration, evapotranspiration, phenology and carbon allocation) that drive the dynamics of terrestrial ecosystems. In this study, we analyse LAI output from five different process-based ecosystem models: CABLE (Wang *et al*., 2010), CLM4 (Lawrence *et al*., 2011), ORCHIDEE (Krinner *et al*., 2005), LPJ (Sitch *et al*., 2003) and VEGAS (Zeng *et al*., 2005). All these models take into account the effects of change in climate and atmospheric CO_2 concentration. The effects of climate change on vegetation growth are generally described through the climatic modification of leaf-level photosynthesis, maintenance respiration and phenology, while change in atmospheric CO_2 concentration influences vegetation growth through photosynthetic rates, water-use efficiency and indirectly, the growing-season length and reproduction. CLM includes nitrogen while CABLE include both nitrogen and phosphorus limitations, therefore effects of increasing nitrogen deposition on vegetation growth can be assessed. These models have been widely used to investigate regional and global terrestrial carbon cycles (Sitch *et al*., 2013), and extensively validated against observations across different ecosystems and regions, including China (Tan *et al*., 2010; Tao & Zhang, 2010; Peng, 2012; Piao *et al*., 2013). Several of these models (e.g., LPJ, ORCHIDEE, and CLM4) have also been applied to detect and attribute change in vegetation growth at the regional and continental scale (Lucht *et al*., 2002; Piao *et al*., 2006; Mao *et al*., 2013; Poulter *et al*., 2013).

All models performed two simulations (S1 and S2) over the period 1901–2009 using historical climate fields from CRU-NCEP v4 dataset (http://dods.extra.cea.fr/data/p529viov/cruncep/) and global atmospheric CO_2 concentration (Keeling and Whorf, 2005, 2009). In simulation S1, models are forced with changing atmospheric CO_2 concentration, while climate is held constant (recycling climate mean and variability from the early decades of the 20th century). Both atmospheric CO_2 concentration and climate are varied in simulation S2. Like previous studies of Lucht *et al.* (2002) and Piao *et al.* (2006), the contributions of atmospheric CO_2 concentration are estimated from the simulation S1, while the effects of climate changes are evaluated based on the difference between simulation S2 and S1. To assess the relative contribution of nitrogen deposition, both CLM4 and CABLE perform another simulation (S3) where atmospheric CO_2 concentration, climate and nitrogen deposition (Bonan & Levis, 2010) are all varied.

To quantify trend of LAI, we perform Linear Least Squares Regression analysis using LAI as dependent variable and year as independent variable. The slope of the regression is then defined as the trend (annual mean increase amount) of LAI.

Results

Spatial patterns of LAI_{GS} trend derived by three satellite datasets

Figure 1 shows spatial patterns of the trend in LAI_{GS} derived from different datasets during the period 1982 to 2009. All satellite-derived observations consistently show that since the 1980s most regions of China have experienced a greening trend, although the magnitude of LAI_{GS} trend is different between the different datasets. The regions with the largest greening trend are generally found in southwest China and part of the North China Plain, where the trend of LAI_{GS} is generally larger than 0.02 yr^{-1}. Overall, GLOBMAP has the largest area exhibiting significant increase in growing-season LAI (56%), followed by GLASS (54%) and GIMMIS (31%).

All three datasets show that LAI_{GS} significantly decrease in less than 5% of the study regions, mainly in northeastern Inner Mongolia, including Xilinguole, and part of the Greater Hinggan mountains. The Yangtze River and the Pearl River deltas also experience a decrease in LAI_{GS}.

Attribution of greening trend at country scale

Figure 2 show trends of LAI_{GS} derived by three satellite datasets and five process-based ecosystem models under different scenario simulations from 1982 to 2009.

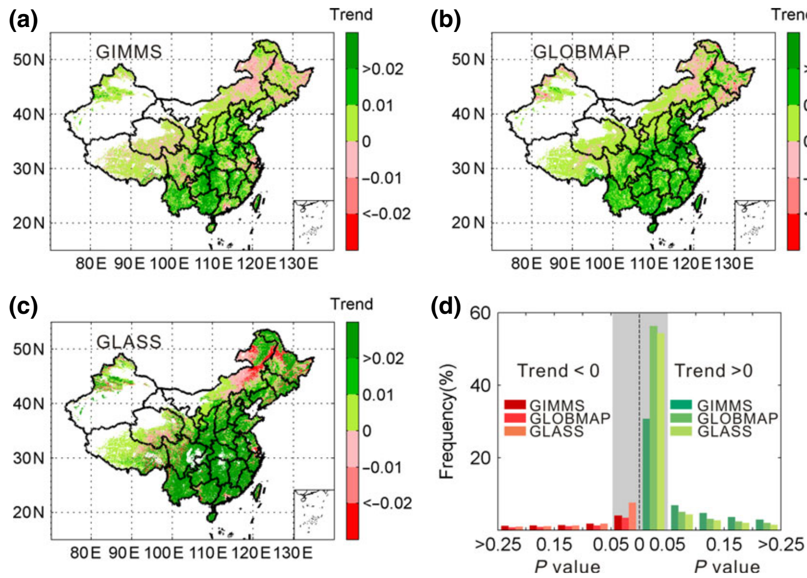

Fig. 1 Spatial distribution of the trend in growing-season (April–October) LAI (LAI_{GS}) during the period 1982–2009. The trends were calculated based on different LAI products: (a), GIMMS dataset; (b) GLOBMAP dataset; (c) GLASS dataset. (d) Frequency distribution of the significance level (P value) of the trends in LAI_{GS} derived by three datasets. The *P* value of the trend in LAI_{GS} for each pixel is estimated based on t test.

All models agree that the effects of CO_2 fertilization resulted in a significantly ($P < 0.05$) increased LAI_{GS}, even though the magnitudes differed from each other. At the country scale, the average trend of LAI_{GS} attributed to rising CO_2 concentration is estimated to be 0.0060 yr^{-1} (ranging from 0.0028 yr^{-1} for ORCHIDEE to 0.0098 yr^{-1} for CABLE), which is about 85% of the average LAI_{GS} trend estimated by satellite datasets (average trend of 0.0070 yr^{-1}, with a range from 0.0035 yr^{-1} to 0.0127 yr^{-1}).

As shown in Fig. 2, the five ecosystem models disagree about the contribution of climate change to the trend of China's LAI_{GS} at the country scale. For example, the VEGAS model shows a significantly positive trend of LAI_{GS} due to the climate change alone, while LAI_{GS} estimated by both CABLE and LPJ is significantly decreased with a trend of −0.0022 yr^{-1} to −0.0050 yr^{-1}, respectively. Insignificant negative trends in LAI_{GS} are also simulated by CLM and ORCHIDEE. The models' estimated average trend of LAI_{GS} in China due to the climate change is about −0.0016 yr^{-1} (ranging from −0.0053 yr^{-1} to 0.0049 yr^{-1}).

For the effects of nitrogen deposition on vegetation growth in China, both CLM and CABLE predict a significant increasing trend of LAI_{GS} at the country scale, although the magnitude of the nitrogen deposition contribution differs between two models: CLM estimates a higher increasing trend of LAI_{GS} (0.0053 yr^{-1}) than CABLE (0.0005 yr^{-1}). Averaging these two model outputs suggests an increasing trend of LAI_{GS} in China

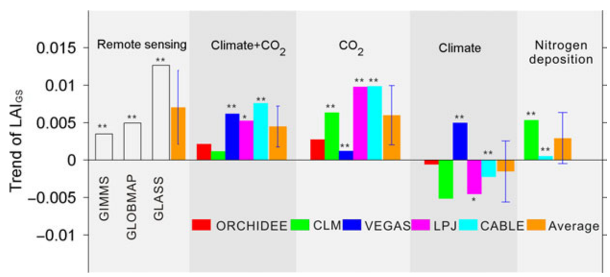

Fig. 2 Trend in China's LAI_{GS} during the period 1982–2009 at the country scale for the three satellite datasets (Remote Sensing) and five process models used. We denote those significant at the 5% level with an asterisk, those significant at the 1% level with two asterisks. Simulation S2 was used to estimate the effect of both change in climate and atmospheric CO_2 concentration on the trend in LAI_{GS} (climate+CO_2), while Simulation S1 was used to estimate the effect of atmospheric CO_2 concentration (CO_2). The contribution of nitrogen deposition is derived by the difference of simulation S3 and simulation S2, while the difference of simulation S2 and simulation S1 was used to estimate contribution of climate change (Climate).

due to nitrogen deposition of about 0.0029 yr^{-1}, which is about 41% of the satellite-observed average trend of LAI_{GS}.

In summary, the combined effect of CO_2 fertilization and climate change (S2 simulation) with the effect of nitrogen deposition, leads to the conclusion that these three factors are responsible for almost all of the average increasing trend of LAI_{GS} observed from the satellites.

Spatial patterns of the trend in LAI_{GS} attributed to different factors

To investigate the spatial patterns of greening trend that can be attributed to the different factors, we estimate the trend in LAI_{GS} for three satellite datasets and from five process-based ecosystem models under different scenario simulations at the provincial scale (Fig. 3). As shown in Fig. 3, the model-estimated contributions of CO_2 fertilization, climate change and nitrogen deposition to the satellite-observed trend of vegetation growth show large spatial heterogeneity across different provinces.

In northern China, including most provinces in the Yellow River basin and northeast China, the average model-estimation shows that climate change alone may reduce LAI_{GS}, accounting for −68% to −150% of the trend in LAI_{GS} in these regions (Fig. 3). Such a negative effect of climate change is comparable or even larger than the positive effects of CO_2 fertilization across most of the regions in northern China. In addition, the attribution of nitrogen deposition to greening trends is also relatively limited (about 8% to 23% of satellite-observed greening trends) in northern China.

Compared to northern China, nitrogen deposition makes a noticeable effect on the trend of satellite-observed LAI_{GS} across most regions of southern China, particularly in the southeast of the country, where the trend of LAI_{GS} attributed to nitrogen deposition is generally larger than 0.0050 yr^{-1}. On the other hand, the relative contribution of climate change and CO_2 fertilization effects on the satellite-derived greening trend in southern China (except Yunnan Province and Hainan Province) is generally smaller than that in the north of the country. For example, the average of model-estimated LAI_{GS} trend due to rising CO_2 concentration (simulation S1) is generally less than 50% of the average trend of LAI_{GS} from the three satellite datasets across most of southern China.

It is unlikely that for most other regions of China, climate change alone significantly increases LAI_{GS} in the Qinghai-Tibet Plateau (Fig. 3). Furthermore, the increasing trend of LAI_{GS} due to climate change is also larger than that driven by rising CO_2 concentration and nitrogen deposition. Note that the contributions of all factors together results in an overestimated LAI_{GS} trend compared to the satellite observations in of the Qinghai-Tibet Plateau.

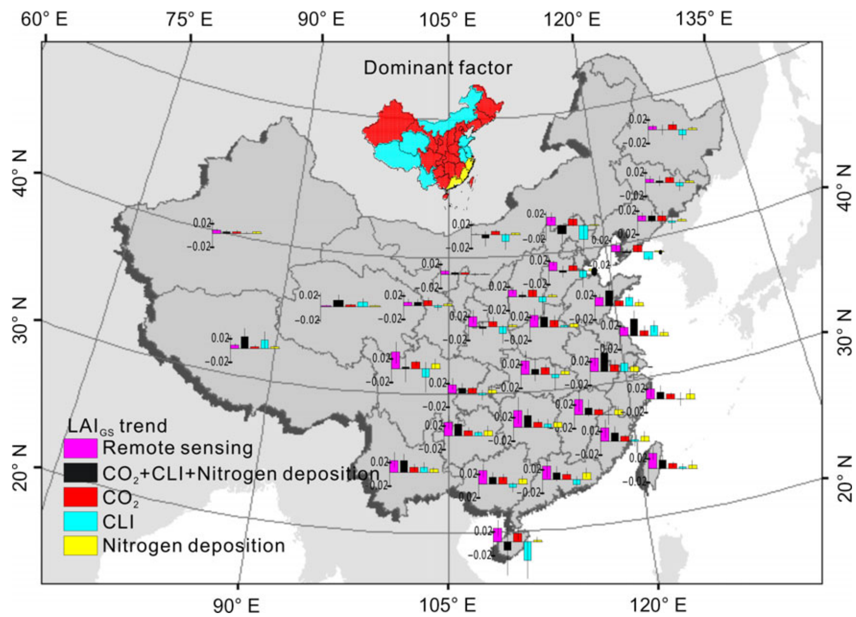

Fig. 3 Trends in LAI_{GS} during the period 1982–2009 at the provincial scale, derived by satellite (Remote Sensing) and process model simulation. Process models estimated average of total effect of rising atmospheric CO_2 concentration, climate change and nitrogen deposition on the trend in LAI_{GS} (CO_2 + CLI + Nitrogen deposition) is estimated based on the sum of average trend in LAI_{GS} from five process models under S2 simulation (considering both change in climate and CO_2 concentration) and average trend in LAI_{GS} due to nitrogen deposition estimated by CLM4 and CABLE model (simulation S3 minus simulation S2). The effects of rising atmospheric CO_2 concentration on the trend in LAI_{GS} (CO_2) is derived from the average of five models under simulation S1, while climate change effect (CLI) is estimated based on the average difference between simulation S2 and S1. The contribution of nitrogen deposition is derived by the CLM4 and CABLE model (simulation S3 minus simulation S2). The inset figure shows the dominant driving factors with the largest trend in LAI_{GS}.

Relationship of LAI_{GS} trend with forest area change and crop yield change

Figure 4 further illustrates the relationship of forest-area change and crop-yield change for each province with the trend of LAI_{GS} as well as the residual of LAI_{GS} trend (RLT) calculated as satellite observation minus model simulation through considering the effects of climate change, rising CO_2 concentration and nitrogen deposition. Note that due to the lack of information on the spatio-temporal change in agricultural management, here, we use change in crop yield. As shown in Fig. 4, provincial forest area change tends to be significantly correlated with the trend of LAI_{GS} ($P < 0.05$), and marginally significantly ($P = 0.07$) correlated with the residual of LAI_{GS} trend, calculated as the trend observed by satellite minus that estimated by models through considering the effects of climate change, rising CO_2 concentration and nitrogen deposition, across different provinces. In contrast, an insignificant correlation of change in crop yield with both trend of LAI_{GS} and RLT is found from the Fig. 4.

Discussion

The reliable detection and attribution of changes in vegetation growth is fundamental to our understanding of the scientific basis of global change, and is needed to enable decision-makers to manage and develop ecosystems in a sustainable way (Hegerl *et al.*, 2010). Compared with the number of studies on the detection of historical trends in vegetation growth under global change, few studies have focused on attribution of the causes of these changes. Commonly, regional vegetation growth changes are the consequence of climate change and anthropogenic changes in atmospheric composition and land use, but it is almost impossible to directly differentiate between these factors (Chen *et al.*, 2014). Using traditional statistical approaches, several previous studies have highlighted the important role of climate change on the change in vegetation growth (Myneni *et al.*, 2007; Zhou *et al.*, 2001; Piao *et al.*, 2004; Peng *et al.*, 2011). For example, Kaufmann *et al.* (2002) applied multiple linear regression using growing-season NDVI as the dependent variable and the corresponding precipitation and temperature as

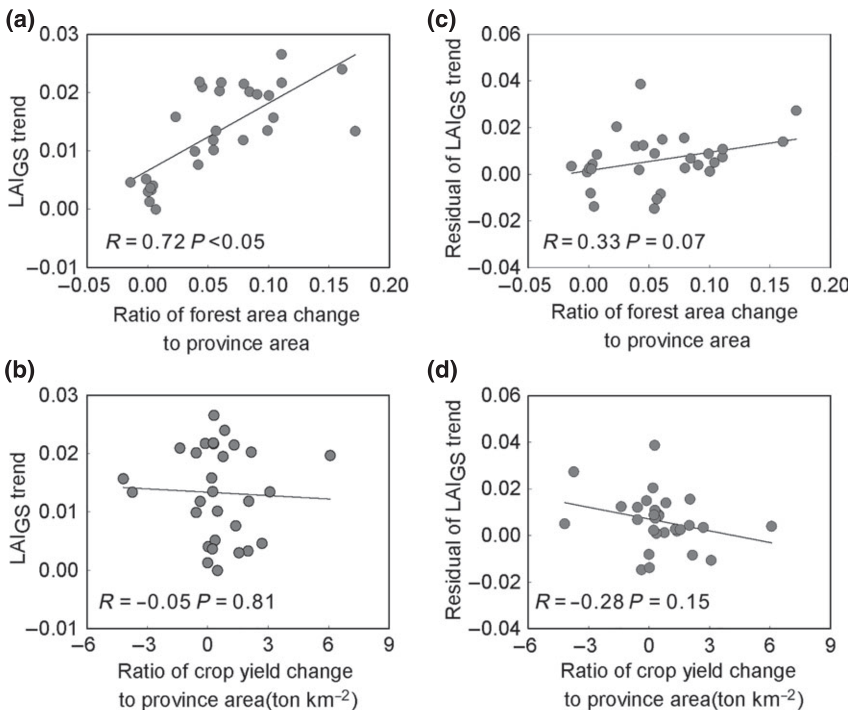

Fig. 4 Relationship of trend in LAI_{GS} and the residual of LAI_{GS} trend (RLT) calculated as satellite observation minus model simulation considering the effects of climate change, rising CO_2 concentration and nitrogen deposition with ratio of forest-area change for each province to the corresponding province area and ratio of crop-yield change for each province to the corresponding province area. (a) Relationship between LAI_{GS} trend and forest-area change; (b) Relationship between LAI_{GS} trend and crop-yield change; (c) Relationship between RLT and forest-area change; (d) Relationship between RLT and crop-yield change.

independent variables. They suggested that global warming was the primary driving force for the enhanced vegetation growth over the Northern Hemisphere. Through considering atmospheric CO_2 concentration as another independent variable in addition to temperature and precipitation, however, Ahlbeck (2002) pointed out that the fertilization effect of rising atmospheric CO_2 concentration was the major contributor to the Northern Hemisphere greening trend. This CO_2 fertilization effect has been demonstrated by Free-Air Carbon dioxide Enrichment (FACE) experiments that show that vegetation productivity is significantly increased in response to rising ambient CO_2 concentration (Norby *et al.*, 2005). Our model estimates suggest that at the country scale, China's greening was chiefly driven by rising atmospheric CO_2 concentration (contributing 85%), although the dominant factor varies across different provinces (Fig. 3).

In this study, we also quantify the contribution of nitrogen deposition to the greening trend in China. Multiple lines of evidence suggest that vegetation growth in the Northern Hemisphere is generally nitrogen-limited (Melillo *et al.*, 2002; Janssens *et al.*, 2010), and the enhanced nitrogen deposition driven by fossil fuel combustion and agricultural fertilization is thought to significantly enhance vegetation growth (Thomas *et al.*, 2009; Fleischer *et al.*, 2013). Our model estimates suggest that current nitrogen deposition contributed about 41% of the satellite-observed average trend of LAI_{GS} at country scale, although this contribution can more clearly be seen in southern China rather than in the north (Fig. 3). This result is consistent with the spatial patterns of the magnitude of nitrogen deposition in China (Jia *et al.*, 2014). Over the last three decades, most of southern China has experienced extensive nitrogen deposition, with typical rates higher than 20 kg ha^{-1} yr^{-1} (Jia *et al.*, 2014). It has been suggested that these high rates of deposition have increased terrestrial ecosystem net carbon uptake in this region (Reay *et al.*, 2008; Yu *et al.*, 2014a). Indeed, evidence has accumulated of significant contributions of subtropical China's land area to the global uptake of anthropogenic CO_2 (Piao *et al.*, 2009; Yu *et al.*, 2014a). For instance, both atmospheric inverse models and inventory data support the postulate that China's terrestrial ecosystem carbon sink is also mainly located in southern China (Piao *et al.*, 2009).

In terms of climate change impact alone, the five models show divergent trends of LAI_{GS} at the country scale. For example, one model (VEGAS) shows a significantly increasing trend, while significantly decreasing trends appears in two other models (CABLE and LPJ). In spite of the discrepancy in trend of LAI_{GS} at the country scale, the models generally agree that climate change alone can result in decreased LAI_{GS} over north China and Inner Mongolia (Fig. 3 and Figure S3). Such negative impacts of climate change are probably driven by the increase in drought in these regions over the past decades (Piao *et al.*, 2010; Peng, 2012; Liu *et al.*, 2013; Yu *et al.*, 2014b). Recent studies based on records of tree-ring widths also suggest that tree growth has declined over the last two decades in Inner Asia due to the growing-season water stress driven by warming-induced increases in atmospheric moisture demand and decreased precipitation (Liu *et al.*, 2013). In contrast, all the models show a positive impact of current climate change on vegetation growth in the Qinghai–Xizang plateau (Fig. 3 and Figure S3), where the most drastic climatic warming has occurred over the past decades (Piao *et al.*, 2010; Yao *et al.*, 2012). Evidence from a field warming experiment has demonstrated that rising temperature can enhance vegetation growth over the plateau (Wang *et al.*, 2012), because vegetation growth in this region is generally limited by the low temperature. It should be noted that for southern China the different models appear to disagree on the impact of climate change on LAI_{GS}. This divergence of model results is due to the different parameterizations of the climate sensitivity of vegetation productivity and soil moisture across different models (Piao *et al.*, 2013). More research is needed to solve this discrepancy.

Additionally, human activities such as afforestation and agricultural management can potentially contribute to the satellite-observed greening in China's vegetation over the last three decades (Pan *et al.*, 2011). Our results show that in 25 of 31 provinces, the average trend of satellite-observed LAI_{GS} is larger than the trend of LAI_{GS} estimated by process models considering the effects of climate change, rising CO_2 concentration and nitrogen deposition (Fig. 3). This effect may be partly explained by activities, such as afforestation. For example, there is a large difference in Hunan province, where forest area has dramatically increased by more than 50% over the last three decades. Furthermore, provincial forest area change tends to be significantly correlated with the trend of LAI_{GS} across different provinces ($P < 0.05$). In addition, there is also marginally significant correlation between the residual of LAI_{GS} trend and change in forest area across different provinces ($P = 0.07$) (Fig. 4). Thus, our results not only highlight the important role of China's afforestation activity in explaining the spatial patterns of trend in vegetation growth, but also strongly suggest that those current carbon cycle models that do not account for land-use change cannot accurately quantify the ecosystem carbon balance in China, particularly in southern China (Piao *et al.*, 2009; Yu *et al.*, 2014a). In addition, despite the spatial correlations between RLT and crop-yield change across different provinces being not statistically significant, there is some evidence that intensive agricultural management is having an effect. For example, in some provinces, such as Hebei and Henan, the effect of climate change, rising CO_2 concentration and nitrogen deposition cannot explain the satellite-observed increase in LAI_{GS}, and relatively high RLT appears. Crop-yield data from the National Agriculture Database (Statistics Bureau of China http://www.stats.gov.cn/tjsj/) suggest that crop yield in these two provinces has increased by more than 6 million tonnes during the study period. Finally, it should be noted that in the Qinghai-Xizang Plateau the satellite-observed increasing trend of LAI_{GS} is smaller than model estimates driven by climate change, rising CO_2 concentration and nitrogen deposition. This negative value of RLT may reveal to a certain extent the negative effects of grazing on the plateau ecosystem (Xie *et al*., 2007; Babel *et al*., 2014), and further studies are required to investigate it.

In summary, to our knowledge, this study is the first to comprehensively detect and attribute a widespread greening trend in China. While some general goals have been achieved, there are a few points that should be addressed in the future. First, both satellite-observed and model-estimated trends of LAI_{GS} show large uncertainties, which are critical when attempting to accurately identify the change in vegetation growth and the contribution of different factors (Hegerl *et al*., 2010). Accordingly, reducing the uncertainties of both satellite observation and model estimation should be the priority of further study. Second, the current study does not fully taken into account the interactions between different factors. For example, only two of the five models consider the effect of nitrogen deposition, although there is increasing evidence that nitrogen limitation strongly decreases the CO_2 fertilization effect (Hickler *et al*., 2008; Norby *et al*., 2010; Piao *et al*., 2013). In addition, the interaction between climate change and rising atmospheric CO_2 is not also considered when estimating contribution of rising atmospheric CO_2 concentration. Finally, the effects of land-use change have not been fully quantified in this study and further work is needed to characterize the roles of changes such as afforestation, agricultural management and grazing. To do so, spatially and temporally explicit historical information needs to be applied to process-based models accounting for forest age, irrigation and grazing management.

Acknowledgements

This study was supported by the National Basic Research Program of China (Grant No. 2013CB956303), Chinese Ministry of Environmental Protection Grant (201209031), National Natural Science Foundation of China (41125004 and 31321061), National Youth Top-notch Talent Support Program in China and the 111 Project (B14001). Jiafu Mao and Xiaoying Shi are supported by the US Department of Energy (DOE), Office of Science, Biological and Environmental Research. Oak Ridge National Laboratory is managed by UT-BATTELLE for DOE under contract DE-AC05-00OR22725. The simulation of CLM is supported by the US Department of Energy (DOE), Office of Science, Biological and Environmental Research. Oak Ridge National Laboratory is managed by UT-BATTELLE for DOE under contract DE-AC05-00OR22725.

References

Ahlbeck JR (2002) Comment on 'Variations in northern vegetation activity inferred from satellite data of vegetation index during 1981–1999' by L. Zhou et al. *Journal of Geophysical Research: Atmospheres*, (1984–2012) **107**, ACH 9-1–ACH 9-2.

Babel W, Biermann T, Coners H *et al.* (2014) Pasture degradation modifies the water and carbon cycles of the Tibetan highlands. *Biogeosciences Discuss*, **11**, 8861–8923.

Berry J, Bjorkman O (1980) Photosynthetic response and adaptation to temperature in higher plants. *Annual Review of Plant Physiology*, **31**, 491–543.

Bonan GB, Levis S (2010) Quantifying carbon-nitrogen feedbacks in the Community Land Model (CLM4). *Geophysical Research Letters*, **37**, L07401.

Chen B, Zhang X, Tao J *et al.* (2014) The impact of climate change and anthropogenic activities on alpine grassland over the Qinghai-Tibet Plateau. *Agricultural and Forest Meteorology*, **189**, 11–18.

Fleischer K, Rebel KT, Molen MK *et al.* (2013) The contribution of nitrogen deposition to the photosynthetic capacity of forests. *Global Biogeochemical Cycles*, **27**, 187–199.

Friedlingstein P, Cox P, Betts R *et al.* (2006) Climate-carbon cycle feedback analysis: results from the C4MIP model intercomparison. *Journal of Climate*, **19**, 3337–3353.

Guo ZD, Hu HF, Li P *et al.* (2013) Spatio-temporal changes in biomass carbon sinks in China's forests from 1977 to 2008. *Science China-Life Sciences*, **56**, 661–671.

Hegerl GC, Hoegh-Guldberg O, Casassa G *et al.* (2010) *Good Practice Guidance Paper on Detection and Attribution Related to Anthropogenic Climate Change*. Meeting Report of the Intergovernmental Panel on Climate Change Expert Meeting on Detection and Attribution of Anthropogenic Climate Change. IPCC Working Group I Technical Support Unit, University of Bern, Bern, Switzerland.

Hickler T, Smith B, Prentice Ic, Mjofors K, Miller P, Arneth A, Sykes Mt. (2008) CO_2 fertilization in temperate FACE experiments not representative of boreal and tropical forests. *Global Change Biology*, **14**, 1531–1542.

Huang Y, Zhang W, Sun W, Zheng X. (2007) Net primary production of Chinese croplands from 1950 to 1999. *Ecological Applications*, **17**, 692–701.

Janssens IA, Dieleman W, Luyssaert S *et al.* (2010) Reduction of forest soil respiration in response to nitrogen deposition. *Nature Geoscience*, **3**, 315–322.

Jia Y, Yu G, He N *et al.* (2014) Spatial and decadal variations in inorganic nitrogen wet deposition in China induced by human activity. *Scientific Reports*, **4**, 3763.

Kaufmann RK, Zhou L, Tucker CJ, Slayback D, Shabanov NV, Myneni RB. (2002) Reply to Comment on 'Variations in northern vegetation activity inferred from satellite data of vegetation index during 1981–1999' by JR Ahlbeck. *Journal of Geophysical Research: Atmospheres* (1984–2012), **107**, ACL 7-1–ACL 7-3.

Keeling CD, Whorf TP (2005, 2009) Atmospheric CO_2 records from sites in the SIO air sampling network. Trends: a compendium of data on global change.

Krinner G, Viovy N, de Noblet-Ducoudré N *et al.* (2005) A dynamic global vegetation model for studies of the coupled atmosphere biosphere system. *Global Biogeochemical Cycles*, **19**, GB1015.

Lawrence DM, Oleson KW, Flanner MG *et al.* (2011) Parameterization improvements and functional and structural advances in version 4 of the Community Land Model. *Journal of Advances in Modeling Earth Systems*, **3**, M03001.

Lee X, Goulden ML, Hollinger DY *et al.* (2011) Observed increase in local cooling effect of deforestation at higher latitudes. *Nature*, **479**, 384–387.

Liu Y, Liu R, Chen JM (2012) Retrospective retrieval of long-term consistent global leaf area index (1981–2011) from combined AVHRR and MODIS data. *Journal of Geophysical Research: Biogeosciences*, **117**, G04003.

Liu H, Park Williams A, Allen CD *et al.* (2013) Rapid warming accelerates tree growth decline in semi-arid forests of Inner Asia. *Global Change Biology*, **19**, 2500–2510.

Lucht W, Prentice IC, Myneni RB *et al.* (2002) Climatic control of the high-latitude vegetation greening trend and Pinatubo effect. *Science*, **296**, 1687–1689.

Mao J, Shi X, Thornton PE, Piao S, Wang X (2012) Causes of spring vegetation growth trends in the northern mid–high latitudes from 1982 to 2004. *Environmental Research Letters*, **7**, 014010.

Mao J, Shi X, Thornton PE, Hoffman FM, Zhu Z, Myneni RB (2013) Global latitudinal-asymmetric vegetation growth trends and their driving mechanisms: 1982–2009. *Remote Sensing*, **5**, 1484–1497.

Melillo JM, Steudler PA, Aber JD *et al.* (2002) Soil warming and carbon-cycle feedbacks to the climate system. *Science*, **298**, 2173–2176.

Myneni RB, Ramakrishna R, Nemani R, Running SW (1997) Estimation of global leaf area index and absorbed PAR using radiative transfer models. *Geoscience and Remote Sensing, IEEE Transactions on*, **35**, 1380–1393.

Myneni RB, Yang W, Nemani RR *et al.* (2007) Large seasonal swings in leaf area of Amazon rainforests. *Proceedings of the National Academy of Sciences of the United States of America*, **104**, 4820–4823.

Nemani RR, Keeling CD, Hashimoto H *et al.* (2003) Climate-driven increases in global terrestrial net primary production from 1982 to 1999. *Science*, **300**, 1560–1563.

Niemand C, Köstner B, Prasse H , Grünwald T, Bernhofer C (2005) Relating tree phenology with annual carbon fluxes at Tharandt forest. *Meteorologische Zeitschrift*, **14**, 197–202.

Norby RJ, DeLucia EH, Gielen B *et al.* (2005) Forest response to elevated CO_2 is conserved across a broad range of productivity. *Proceedings of the National Academy of Sciences of the United States of America*, **102**, 18052–18056.

Norby RJ, Warren JM, Iversen CM, Medlyn BE, McMurtrie RE (2010) CO_2 enhancement of forest productivity constrained by limited nitrogen availability. *Proceedings of the National Academy of Sciences of the United States of America*, **107**, 19368–19373.

Oleson KW, Bonan GB, Feddema J, Vertenstein M, Kluzek E (2010) *Technical Description of an Urban Parameterization for the Community Land Model (CLMU)*. NCAR, Boulder.

Pan Y, Birdsey RA, Fang J *et al.* (2011) A large and persistent carbon sink in the world's forests. *Science*, **333**, 988–993.

Peng S (2012) Global change impacts on forest ecosystems in East Asia. PhD Thesis. Peking University, China.

Peng S, Chen A, Xu L *et al.* (2011) Recent change of vegetation growth trend in China. *Environmental Research Letters*, **6**, 044027.

Peng S, Piao S, Shen Z *et al.* (2013) Precipitation amount, seasonality and frequency regulate carbon cycling of a semi-arid grassland ecosystem in Inner Mongolia, China: a modeling analysis. *Agricultural and Forest Meteorology*, **178**, 46–55.

Peng S, Piao S, Zeng Z *et al.* (2014) Afforestation in China cools local land surface temperature. *Proceedings of the National Academy of Sciences of the United States of America*, **111**, 2915–2919.

Piao S, Fang J, Zhou L *et al.* (2003) Interannual variations of monthly and seasonal normalized difference vegetation index (NDVI) in China from 1982 to 1999. *Journal of Geophysical Research: Atmospheres*, **108**, 4401.

Piao S, Fang J, Ji W, Guo Q, Ke J, Tao S (2004) Variation in a satellite-based vegetation index in relation to climate in China. *Journal of Vegetation Science*, **15**, 219–226.

Piao S, Friedlingstein P, Ciais P, Zhou L, Chen A (2006) Effect of climate and CO2 changes on the greening of the Northern Hemisphere over the past two decades. *Geophysical Research Letters*, **33**, L23402.

Piao SL, Friedlingstein P, Ciais P, Viovy N, Demarty J (2007) Growing season extension and its effects on terrestrial carbon flux over the last two decades. *Global Biogeochemical Cycles*, **21**, GB3018.

Piao SL, Ciais P, Friedlingstein P *et al.* (2008) Net carbon dioxide losses of northern ecosystems in response to autumn warming. *Nature*, **451**, 49–52.

Piao S, Fang J, Ciais P *et al.* (2009) The carbon balance of terrestrial ecosystems in China. *Nature*, **458**, 1009–1013.

Piao S, Ciais P, Huang Y *et al.* (2010) The impacts of climate change on water resources and agriculture in China. *Nature*, **467**, 43–51.

Piao S, Sitch S, Ciais P *et al.* (2013) Evaluation of terrestrial carbon cycle models for their response to climate variability and to CO_2 trends. *Global Change Biology*, **19**, 2117–2132.

Piao S, Nan H, Huntingford C, *et al.* (2014) Evidence for a weakening relationship between interannual temperature variability and northern vegetation activity. *Nature communications*, **5**, 1–7.

Poulter B, Pederson N, Liu H *et al.* (2013) Recent trends in Inner Asian forest dynamics to temperature and precipitation indicate high sensitivity to climate change. *Agricultural and Forest Meteorology*, **178**, 31–45.

Reay DS, Dentener F, Smith P, Grace J, Feely RA (2008) Global nitrogen deposition and carbon sinks. *Nature Geoscience*, **1**, 430–437.

Sitch S, Smith B, Prentice IC *et al.* (2003) Evaluation of ecosystem dynamics, plant geography and terrestrial carbon cycling in the LPJ dynamic global vegetation model. *Global Change Biology*, **9**, 161–185.

Sitch S, Huntingford C, Gedney N *et al.* (2008) Evaluation of the terrestrial carbon cycle, future plant geography and climate-carbon cycle feedbacks using five Dynamic Global Vegetation Models (DGVMs). *Global Change Biology*, **14**, 2015–2039.

Sitch S, Friedlingstein P, Gruber N *et al.* (2013) Trends and drivers of regional sources and sinks of carbon dioxide over the past two decades. *Biogeosciences Discussion*, **10**, 20113–20177.

Tan K, Ciais P, Piao S *et al.* (2010) Application of the orchidee global vegetation model to evaluate biomass and soil carbon stocks of Qinghai Tibetan grasslands. *Global Biogeochemical Cycles*, **24**, GB1013.

Tao F, Zhang Z (2010) Dynamic responses of terrestrial ecosystems structure and function to climate change in China. *Journal of Geophysical Research: Biogeosciences*, **115**, G03003.

Thomas RQ, Canham CD, Weathers KC, Goodale CL (2009) Increased tree carbon storage in response to nitrogen deposition in the US. *Nature Geoscience*, **3**, 13–17.

Wang YP, Law RM, Pak B (2010) A global model of carbon, nitrogen and phosphorus cycles for the terrestrial biosphere. *Biogeosciences*, **7**, 2261–2282.

Wang S, Duan J, Xu G *et al.* (2012) Effects of warming and grazing on soil N availability, species composition, and ANPP in an alpine meadow. *Ecology*, **93**, 2365–2376.

Xiao Z, Liang S, Wang J, Chen P, Yin X, Zhang L, Song J (2014) Use of general regression neural networks for generating the GLASS leaf area index product from time-series MODIS surface reflectance. *Geoscience and Remote Sensing, IEEE Transactions on*, **52**, 209–223.

Xie Y, Becker U, Wittig R (2007) Vegetation of the Stipa loess steppe in Ningxia (northern China) in relation to grazing intensity. *Grassland Science*, **53**, 143–154.

Xu L, Myneni RB, Chapin FS III *et al.* (2013) Temperature and vegetation seasonality diminishment over northern lands. *Nature Climate Change*, **3**, 581–586.

Yamori W, Hikosaka K, Way DA (2014) Temperature response of photosynthesis in C3, C4, and CAM plants: temperature acclimation and temperature adaptation. *Photosynthesis Research*, **119**, 101–117.

Yao T, Thompson L, Yang W *et al.* (2012) Different glacier status with atmospheric circulations in Tibetan Plateau and surroundings. *Nature Climate Change*, **2**, 663–667.

Yu G, Chen Z, Piao S *et al.* (2014a) High carbon dioxide uptake by subtropical forest ecosystems in the East Asian monsoon region. *Proceedings of the National Academy of Sciences of the United States of America*, **111**, 4910–4915.

Yu M, Li Q, Hayes MJ, Svoboda MD, Heim RR (2014b) Are droughts becoming more frequent or severe in China based on the standardized precipitation evapotranspiration index: 1951–2010. *International Journal of Climatology*, **34**, 545–558.

Zeng N, Qian H, Roedenbeck C, Heimann M (2005) Impact of 1998–2002 midlatitude drought and warming on terrestrial ecosystem and the global carbon cycle. *Geophysical Research Letters*, **32**, L22709.

Zhou L, Tucker CJ, Kaufmann RK, Slayback D, shabanov NV, Myneni RB (2001) Variations in northern vegetation activity inferred from satellite data of vegetation index during 1981 to 1999. *Journal of Geophysical Research: Atmospheres*, **106**, 20069–20083.

Zhu Z, Bi J, Pan Y *et al.* (2013) Global data sets of vegetation leaf area index (LAI) 3 g and Fraction of Photosynthetically Active Radiation (FPAR) 3 g derived from Global Inventory Modeling and Mapping Studies (GIMMS) Normalized Difference Vegetation Index (NDVI3 g) for the period 1981 to 2011. *Remote Sensing*, **5**, 927–948.

Supporting Information

Additional Supporting Information may be found in the online version of this article:

Figure S1. Spatial distribution of province administrations in China.
Figure S2. Trend of three different satellite-derived LAI_{GS} across different provinces during the period 1982–2009. (a), GIMMS LAI dataset; (b) GLOBMAP LAI dataset; (c) GLASS LAI dataset.
Figure S3. Trend of process model-estimated LAI_{GS} in response to change in climate, rising atmospheric CO_2 concentration, and nitrogen deposition, across different provinces during the period 1982–2009.